JOURNAL OF GEOPHYSICAL RESEARCH: OCEANS, VOL. 118, 1–11, doi:10.1002/jgrc.20337, 2013

Intrathermocline eddies in the coastal transition zone off central Chile (31–41°S)

Samuel Hormazabal,[1] Vincent Combes,[2] Carmen E. Morales,[3] Marco A. Correa-Ramirez,[1] Emmanuel Di Lorenzo,[4] and Sergio Nuñez[5]

Received 16 January 2013; revised 2 August 2013; accepted 5 August 2013.

[1] The three-dimensional structure and the origin of mesoscale anticyclonic intrathermocline eddies (ITEs) in the coastal transition zone (CTZ) off central Chile (31–41°S) were analyzed through the combination of data from oceanographic cruises and satellite altimetry, and the application of an eddy-resolving primitive equation ocean model coupled with a numerical experiment using a passive tracer. In this region, ITEs are represented by subsurface lenses (~100 km diameter; 500 m thickness or vertical extension) of nearly homogeneous salinity (>34.5) and oxygen-deficient (<1.0 mL L^{-1}) waters, properties which are linked to the equatorial subsurface water mass (ESSW) transported poleward by the Peru-Chile undercurrent (PCUC) in the coastal band. At least five to seven ITEs were observed simultaneously in the area between 31° and 38°S during winter cruises in 1997 and 2009. Satellite data indicated that the ITEs identified from in situ data moved westward, each at a mean speed of ~2 km d^{-1} and transported a total volume of ~1 × 10^6 m^3 s^{-1} (=1 Sv); the lifespan of each ITE ranged from a few months to 1 year. Model results indicate that ITEs become detached from the PCUC under summer upwelling conditions in the coastal zone.

Citation: Hormazabal, S., V. Combes, C. E. Morales, M. A. Correa-Ramirez, E. Di Lorenzo, and S. Nuñez (2013), Intrathermocline eddies in the coastal transition zone off central Chile (31–41°S), *J. Geophys. Res. Oceans*, *118*, doi:10.1002/jgrc.20337.

1. Introduction

[2] A special group of ocean mesoscale eddies, the intrathermocline eddies (ITEs), is characterized by having its core in subsurface waters and within the thermocline, sometimes with a reduced expression at the sea surface [*Dugan et al*., 1982; *Gordon et al*., 2002]. ITEs are vortices or lenses of relatively homogeneous water, with similar characteristics to the water in their formation area but distinct from that in the surrounding thermocline water [*Kostianoy and Belkin*, 1989; *Nauw et al*., 2006; *Johnson and McTaggart*, 2010]. Typically, ITEs have a dome shape in the shallower section (upper thermocline) and a bowl shape (concave) in the deeper section (lower thermocline); most of them have an anticyclonic rotation due to the dominance of the depression of the lower thermocline [*Kostianoy and Belkin*, 1989; *Gordon et al*., 2002; *McGillicuddy et al*., 2007; *Filyushkin and Stovoloskiy*, 2011]. ITEs have been observed in several regions of the oceans [*Kostianoy and Belkin*, 1989], including the North Atlantic, associated to the Mediterranean outflow waters (Meddies) [*McDowell and Rossby*, 1978; *Richardson et al*., 2000]; the Indian Ocean, associated to the Red Sea outflow water (Reddies) [*Shapiro and Meschanov*, 1991]; the eastern North Pacific Ocean, associated to the California undercurrent (Cuddies) [*Simpson and Lynn*, 1990; *Garfield et al*., 1999; *Jerónimo and Gómez-Valdés*, 2007]; the Japan/East Sea associated to the Japan/East Sea subpolar front [*Gordon et al*., 2002]; and, most recently, the eastern South Pacific Ocean, associated with 13°C waters [*Johnson and McTaggart*, 2010; *Chaigneau et al*., 2011]. Unlike surface eddies, ITEs strongly influence the intermediate or deeper layers in the oceans; in these terms, they could have a larger contribution in the spreading rates and pathways of water masses and, with it, can play an important role in salt and heat fluxes in the oceans as it has been described for mesoscale eddies in general [*Ballegooyen et al*., 1994; *Treguier et al*., 2012]. The impact that ITEs have on the productivity of pelagic systems in the CTZ or the open ocean has been analyzed in a few studies [e.g., *McGillicuddy et al*., 2007; *Hansen et al*., 2010; *Morales et al*., 2012].

[3] Eastern boundary current systems have been characterized as areas where mesoscale eddies are recurrent features in the CTZ and open ocean, as detected from satellite altimetry [*Hormazabal et al*., 2004; *Capet et al*., 2008; *Chaigneau et al*., 2009, 2011]. However, the type of eddy (surface or subsurface) cannot be assessed from altimetry

[1]Escuela de Ciencias del Mar, Pontificia Universidad Católica de Valparaíso, Valparaíso, Chile.
[2]College of Oceanic and Atmospheric Sciences, Oregon State University, Corvallis, Oregon, USA.
[3]Departamento de Oceanografía, Universidad de Concepción, Concepción, Chile.
[4]School of Earth and Atmospheric Sciences, Georgia Institute of Technology, Atlanta, Georgia, USA.
[5]Instituto de Investigación Pesquera de la 8° Región, Talcahuano, Chile.

Corresponding author: S. Hormazabal, Escuela de Ciencias del Mar, Pontificia Universidad Católica de Valparaíso, PO Box 1020, Valparaíso, Chile. (samuel.hormazabal@ucv.cl)

2169-9275/13/10.1002/jgrc.20337

alone because they display the same type of vorticity [*Colas et al*., 2012]; the combination of satellite and in situ data is required to resolve this uncertainty and to characterize their three-dimensional structure. In the California and Canary Current Systems, large segments of the poleward undercurrent detach from the continental slope and form anticyclonic ITEs (∼100 km diameter) that transport warm and salty waters from the CTZ to the open ocean [*Richardson et al*., 2000; *Jerónimo and Gómez-Valdés*, 2007]. Using these results, *Johnson and McTaggart* [2010] suggested that ITEs in the Chile-Peru region (eastern South Pacific Ocean) originated in the area of the Peru-Chile undercurrent (PCUC). The PCUC flows poleward, at depths between 100 and 400 m (core at ∼220 m depth), along the coast of Peru (∼6°S) to the Gulf of Penas (Chile; 48°S) and transports Equatorial Subsurface Waters (ESSW) [*Silva and Neshyba*, 1979]. This water mass is characterized by a subsurface salinity maximum (34.2–34.6), relatively warm subsurface waters, low oxygen concentrations (<3 mL L^{-1}), and high nutrient concentrations [*Silva et al*., 2009]. Off central Chile, the ESSW constitutes the main source of nutrient input to the photic layer during wind-driven upwelling events, stimulating large increases in phytoplankton biomass and primary production in the coastal zone [*Strub et al*., 1998; *Morales et al*., 2007]. The transport of nutrients away from the coastal upwelling zone and into the CTZ via eddies, including ITEs, has been argued to be a mechanism by which the pelagic production in the coastal band might be negatively affected, as evaluated with model simulations [*Gruber et al*., 2011]. In this context, this study focuses on the description of the three-dimensional structure of ITEs off central Chile (section 3.1) and on the distinction of ITEs from low-frequency internal waves and areas where ITEs are formed in this region (section 3.2), using a combination of data obtained from satellite altimetry and hydrographic cruises. The origin of ITEs off central Chile was also explored with the application of an eddy-resolving primitive equation ocean model coupled with a numerical experiment using a passive tracer (section 3.3). The potential impacts of ITEs on the pelagic system in the CTZ and the coastal upwelling area in the eastern South Pacific region, one of the most productive in the world oceans, are discussed (section 3.4).

2. Data and Methods

2.1. Satellite Altimetry Data

[4] Sea level anomaly (SLA) satellite data for the region off central Chile (31–41°S) were obtained from a grid (0.25° × 0.25° resolution) every 7 days during the 1997–2009 period, using a combined processing of TOPEX/Jason/ERS altimeter data distributed by AVISO (http://aviso.oceanobs.com). These SLA data were used to obtain the surface geostrophic velocity field [see *Hormazabal et al*., 2004] and, in addition, to identify the time and location of eddy formation and to define their main characteristics (size, age, speed, direction of movement, etc.). Eddy identification was based on the Okubo-Weiss (W) parameter [*Isern-Fontanet et al*., 2004], which allows the detection of vorticity-dominated areas where W is <-0.2 SDw, the spatial standard deviation of W. The Okubo-Weiss parameter evaluates the relative dominance of strain and vorticity:

$$W = s_s^2 + s_n^2 - \omega^2$$

where s_s and s_n are the normal and shear components of strain:

$$s_s = \partial V_g/\partial x + \partial U_g/\partial y$$

$$s_n = \partial U_g/\partial x - \partial V_g/\partial y$$

and $\omega = \partial V_g/\partial x - \partial U_g/\partial y$ is the relative vorticity, where U_g and V_g correspond to east-west and north-south components of the surface geostrophic velocity, respectively.

[5] A threshold value of -5×10^{-12} s^{-2} was used to identify coherent structures from the background field (features <50 km diameter were not considered), and the vorticity sign (− or +) in their centers were used to define the type of eddy (cyclonic or anticyclonic, respectively), as explained in *Correa-Ramirez et al*. [2007].

2.2. Hydrographic Data

[6] Vertical sections (0–600 m depth) of temperature, salinity, sigma-t, oxygen, and fluorescence were obtained with a CTD (Conductivity-Temperature-Depth profiler, model Sea Bird SBE-25, SBE-19, and Niels Braun Mark III), equipped with dissolved oxygen and fluorescence sensors, during four different oceanographic cruises (Figures 1–3) for the "Fondo de Investigación Pesquera (FIP). Three cruises were carried out on board RV Abate Molina, FIP 96-13 (CTD Niels Braun Mark III Romano), FIP 97-12 (CTD Niels Braun Mark III Romano), and FIP 2007-16 (CTD Sea Bird-19); a fourth (FIP 2008-20) was carried out on board RV Agor Vidal Gormáz (CTD Sea Bird SBE-25). Cross-shore CTD sections were obtained during the austral fall for FIP 96-13 (section at 37°20′ on 20–21 May 1997) and summer for FIP 2008-20 (section at 36°30′S on 6–13 January 2009); the stations in these sections were separated by <0.3° (Figures 1–3). Alongshore CTD sections (following the continental shelf margin: ∼500 m depth isobath), located between 31° and 41°S and involving 20 CTD stations separated by ∼0.5° of latitude (Figures 1 and 4), were obtained during the austral winter for FIP 97-12 (2 August to 8 September 1997) and FIP 2007-16 (18 July to 22 August 2007). In addition, discrete water samples for oxygen and salinity analyses were collected with a rosette equipped with Niskin bottles and were used for the subsequent data correction obtained from the CTD sensors. The methods used in the analyses of salinity and dissolved oxygen samples have been described in detail in previous works [*Morales et al*., 2007].

[7] ITEs observed in the cross-shore hydrographic sections were then identified with satellite altimetry and were followed backward and forward in time to detect their initial surface expression and their disappearance (= eddy's lifespan). The uncertainty in ITEs lifespan estimates is of ∼1 week (the time interval between each altimetry satellite data); however, their lifespan could be underestimated if their surface signal becomes undetectable by altimetry at any one time. In order to estimate the volume of water transported by these ITEs, eddy surface scales obtained by altimetry (W parameter) and eddy vertical scales obtained

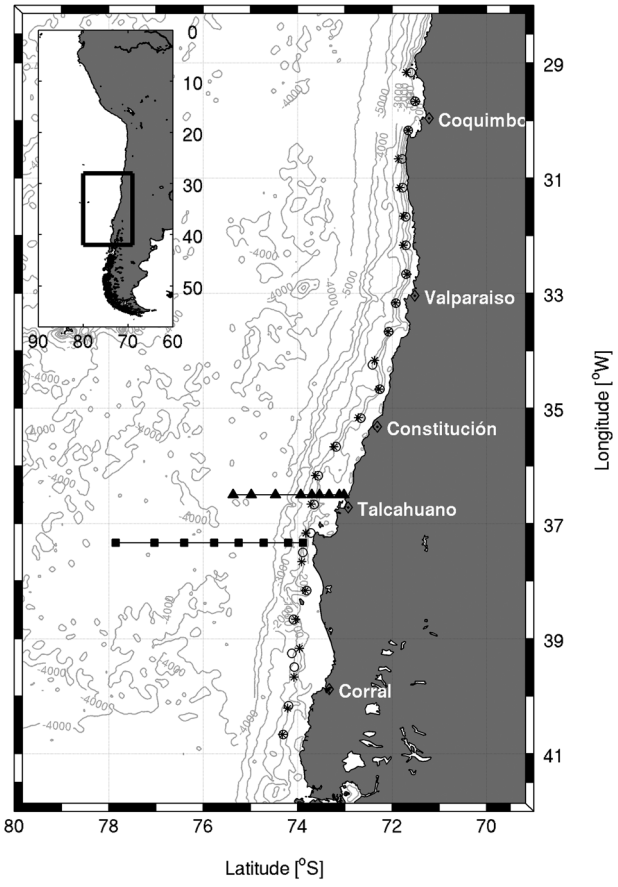

Figure 1. Bathymetry of the study area in the eastern South Pacific Ocean. Also shown are the positions of the hydrographic cross-shore sections during the oceanographic cruise carried out during: austral fall of 1997 (20–23 May; filled square), austral summer of 2009 (8–16 January; filled triangle), and hydrographic alongshore sections (31–41°S) during the oceanographic cruise carried out during the austral winter in 1997 (2 August to 8 September; white dots) and 2007 (18 July to 22 August; star).

by hydrographic cross-shore sections were used (see Figures 2 and 3).

2.3. Model Setup

[8] The Regional Ocean Modeling System (ROMS) was used to investigate the origin of ITEs off central Chile. ROMS is a free-surface, hydrostatic, eddy-resolving primitive equation ocean model that uses stretched, terrain-following coordinates in the vertical and orthogonal curvilinear coordinates in the horizontal [*Haidvogel et al*., 2000; *Shchepetkin and McWilliams*, 2005]. The model grid extends westward from 70°W to 85°W and northward from 40°S to 25°S (white frame on Figure 5a). The grid has an average spatial resolution of ∼4.6 km and 40 vertical levels, with enhanced resolution near the surface (specified by the ROMS stretching parameters (θb, θs, hc) = (0, 6, 10 m)). The bathymetry is a smoothed version of the ETOPO2 (2′ resolution) gridded data to avoid large pressure gradient errors [*Mellor et al*., 1994]. The initial and monthly averaged boundary conditions (using a modified radiation boundary condition from *Marchesiello et al*. [2001] from 2000 to 2008 are obtained from a high-resolution (10 km) MOM3-based Ocean General Circulation Model (OGCM) code optimized for the Earth Simulator (OFES) [*Masumoto et al*., 2004; *Sasaki et al*., 2004, 2006]. At the surface, the heat and freshwater fluxes are a monthly mean climatology derived from the Comprehensive Ocean-Atmosphere Data Set (COADS) data set [*da Silva et al*., 1994]. The model momentum flux is a daily averaged wind stress from the QuickSCAT data set from 2000 to 2008. To track the water originated in the Peru-Chile undercurrent, a model passive tracer, following an advection-diffusion equation, as in *Combes et al*. [2009] (no decay term), was released continuously during the year 2007 off Valparaiso and in the subsurface (between 100 and 350 m depth; green rectangle on Figure 5a).

3. Results and Discussion

3.1. Identification and Characterization of ITEs Off Central Chile

[9] The geostrophic surface current field in the CTZ off central Chile, as derived from satellite altimetry, revealed the presence of a strong meandering current and several cyclonic and anticyclonic mesoscale eddies during the oceanographic cruises carried out in the austral fall of 1997 (Figure 2) and summer of 2009 (Figure 3). Mesoscale eddies in this CTZ have been detected from satellite altimetry alone [*Cáceres*, 1992; *Hormazabal et al*., 2004] and from a combination of satellite altimetry and hydrographic data [*Morales et al*., 2007, 2010; *Letelier et al*., 2009]; numerical models for the region have also identified them [*Leth and Middleton*, 2004; *Colas et al*., 2012; *Chaigneau et al*., 2011]. Only recently, however, eddies of the ITE type have been detected in this region, using Argo float profiles [*Johnson and McTaggart*, 2010], a combination of satellite altimetry and Argo floats [*Chaigneau et al*., 2011], or satellite altimetry and hydrographic data [*Morales et al*., 2012]. The present study provides further insights on the three-dimensional characteristics of ITEs by using a combination of satellite altimetry, hydrographic data, and modeling.

[10] During the fall 1997 and summer 2009 cruises, some of the cross-shore hydrographic sections (36°30′S and 37°20′S, respectively) crossed through mesoscale anticyclonic eddies of the ITE type (Figures 2b–2d and 3b–3d). In these two sections, lenses of high salinity (>34.5) and low dissolved oxygen concentration (<1.0 mL L^{-1}), characteristics associated to the ESSW water transported by the PCUC in this region, were observed beyond the continental shelf and slope areas (Figures 2f–2g and 3f–3g). The distributions of temperature and density (sigma-pot) also displayed a lens shape (Figures 2e and 2g and Figures 3e and 3g), as did the fluorescence signal (Figures 2i and 3i); these characteristics, together with a higher fluorescence within the lenses, were clearly distinguishable from the surrounding thermocline waters. These ITEs had a horizontal diameter (based on satellite altimetry) of ∼100 km and a thickness (vertical extension between the upper and lower limit of the eddy, based on CTD data) of ∼500 m (Table 1). The diameter was similar but the thickness was at least 2 to 3 times larger compared with the ITEs reported by *Gordon et al*. [2002] and *Nauw et al*. [2006]; however,

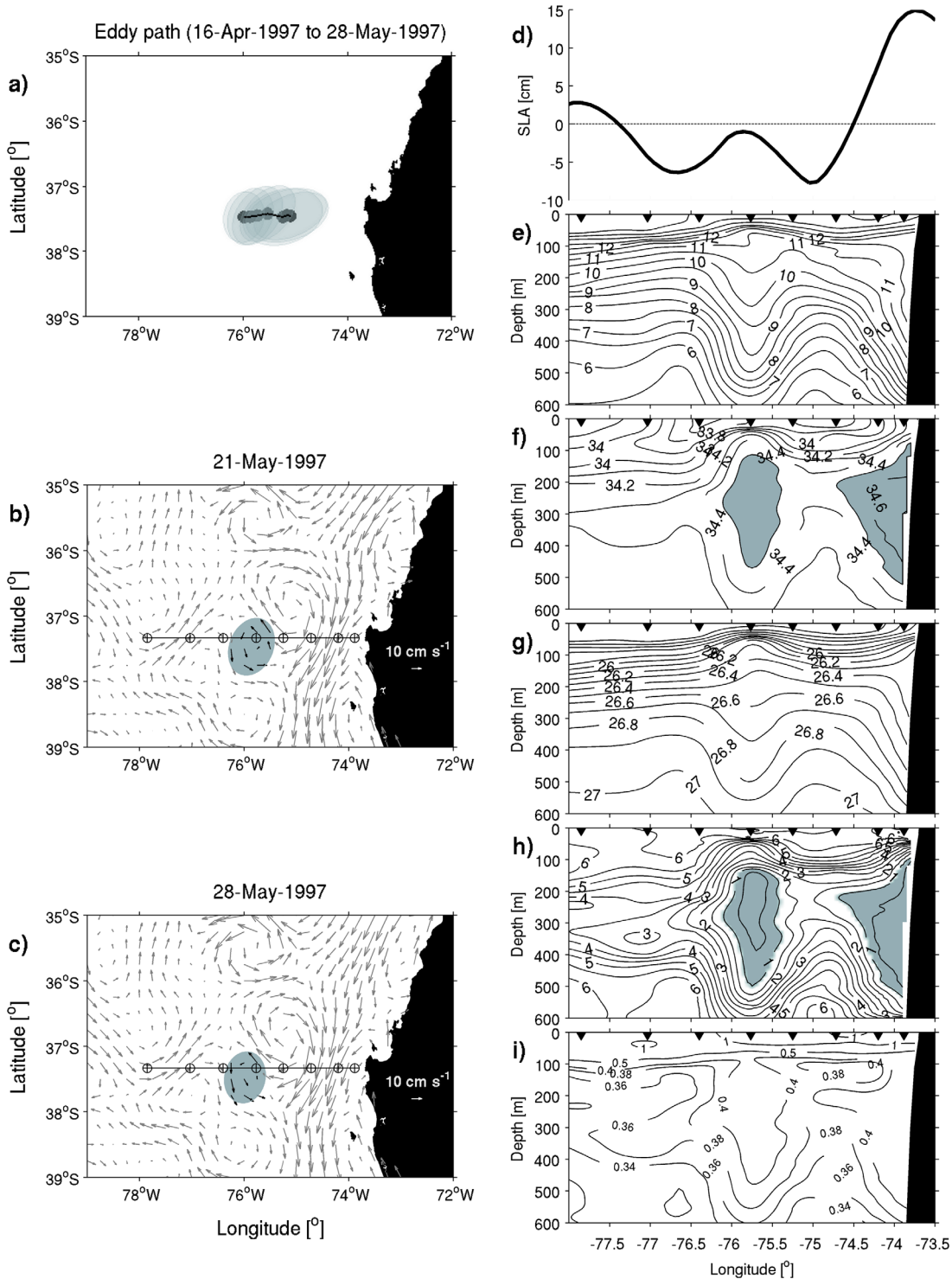

Figure 2. Satellite SLA and cross-shore hydrographic sections during the oceanographic cruise carried out during the austral fall of 1997 (20–23 May): (a) eddy path and history based on SLA data; surface geostrophic currents during (b) 19 May and (c) 29 May; (d) SLA profile along the transect 37°20′S, represented also by a continuous straight line in Figures 2b and 2c; and vertical profiles of (e) temperature (°C), (f) salinity, (g) density (sigma-pot), (h) dissolved oxygen (mL L^{-1}), and (i) fluorescence (relative units). The positions of the hydrographic stations are indicated by open circles (Figures 2b and 2c) and triangles (Figures 2e–2i).

Martin and Richards [2001] have reported ITEs with thicknesses >1000 m. Overall, ITEs in the CTZ could contribute to a significant water transport from the coastal upwelling zone toward the oligotrophic region in the subtropical gyre of the South Pacific [*Johnson and McTaggart*, 2010].

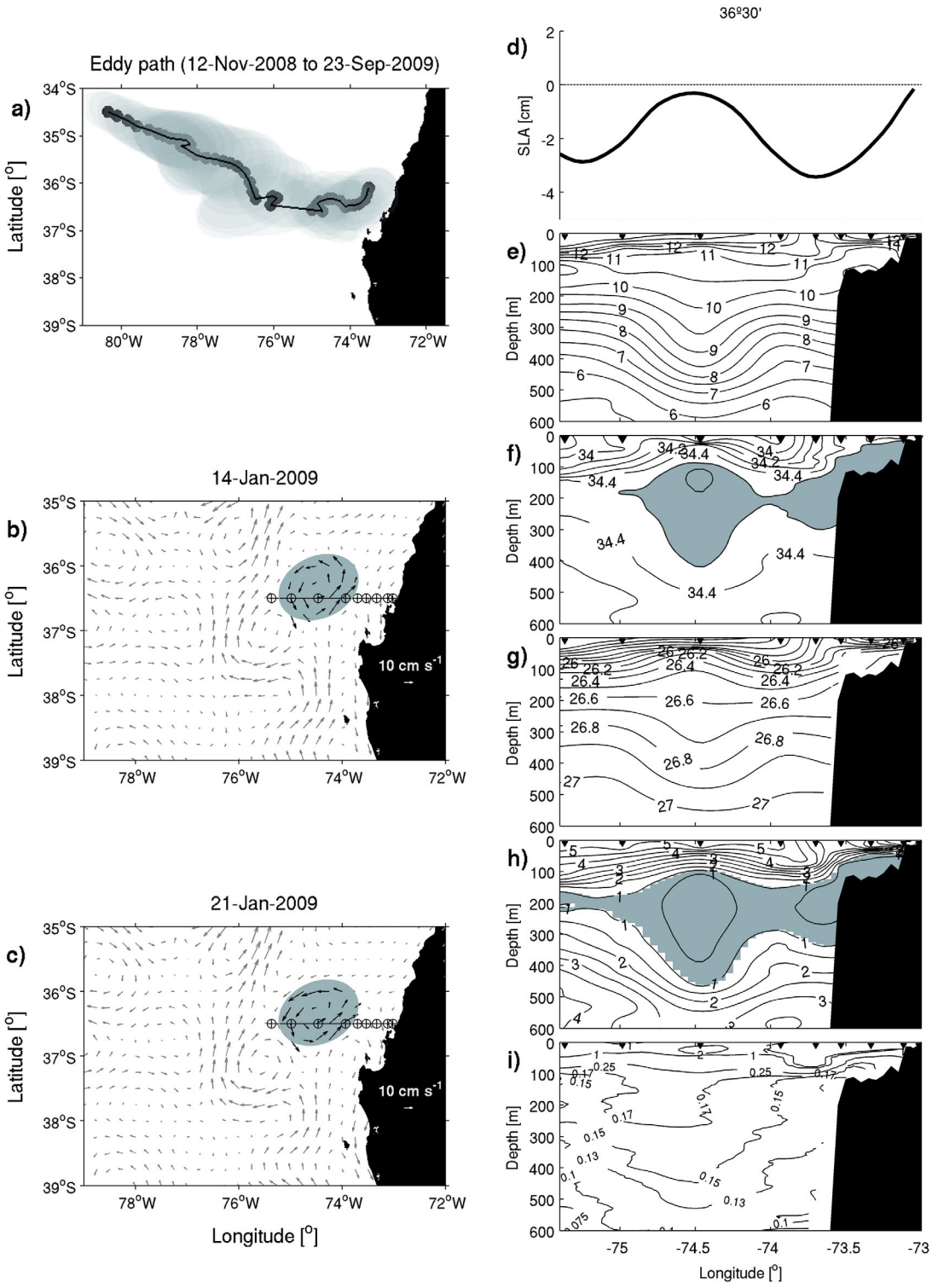

Figure 3. Satellite SLA and cross-shore hydrographic section during the oceanographic cruise carried out during the austral summer of 2009 (8–16 January): (a) eddy path and history based on SLA data; surface geostrophic currents during (b) 14 January and (c) 21 January; (d) SLA profile along the transect 36°30′S, represented also by a continuous straight line in Figures 3b and 3c; and vertical profiles of (e) temperature (°C), (f) salinity, (g) density (sigma-pot), (h) dissolved oxygen (mL L^{-1}), and (i) fluorescence (relative units). The positions of the hydrographic stations are indicated by open circles (Figures 3b and 3c) and triangles (Figures 3e–3i).

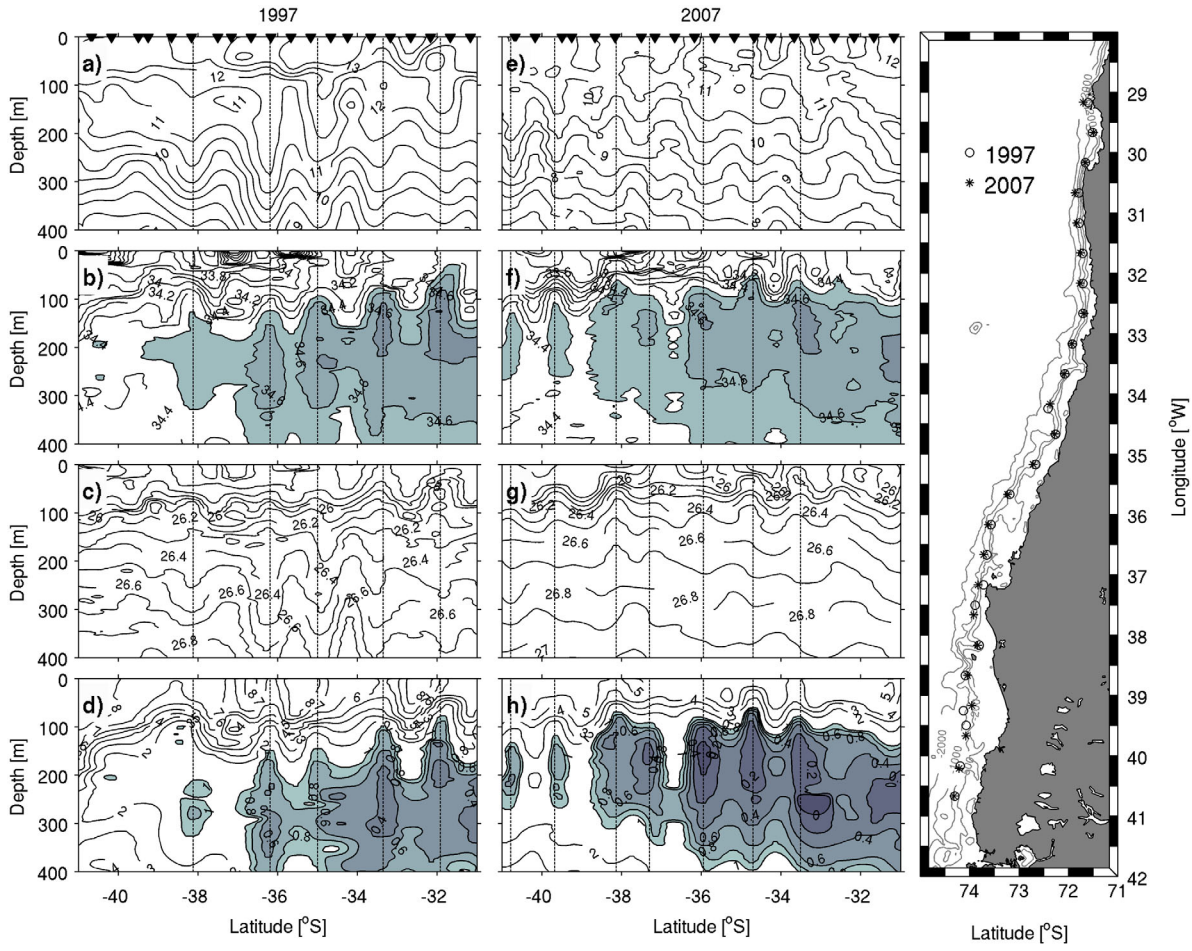

Figure 4. Alongshore hydrographic sections (31–41°S) during the oceanographic cruise carried out during the austral winter in 1997 (2 August to 8 September) and 2007 (18 July to 22 August). Vertical profiles of (a and e) temperature (°C), (b and g) salinity, (c and g) density (sigma-pot), and (d and h) dissolved oxygen (mL L^{-1}), for 1997 and 2007) cruises, respectively. Vertical line indicates the location of the ITEs. Positions of hydrographic stations for 1997 (white dots) and 2007 (star) cruise (right panel).

[11] After the detection of ITEs with hydrographic data, their history was reconstructed based on SLA and W analyses using satellite data. The results indicated that these structures were generated close to the coastal zone (at depths >500 m). The ITE identified during the 1997 fall cruise was first detected by satellite on 16 April, a month before the oceanographic cruise, and it was located off Punta Lavapié at 37.5°S (Figure 2a). The one identified during the 2009 summer cruise first appeared on 12 November, about 2 months before the cruise, and it was located north of Concepcion at 36°S (Figure 3a). Apparently, the 1997 ITE had a relatively short duration (∼49 d) compared with the 2009 ITE (∼322 d). Also, the 2009 ITE had a surface area about ∼40% larger than the 1997 ITE, but other characteristics (depth of the boundaries, thickness, vorticity, and velocity) were relatively similar between both structures (Table 1). Differences in the characteristics of ITEs in the study region could be associated with changes in wind forcing and in PCUC vorticity. The intensification of coastal upwelling generates an increase in the offshore density gradient, introducing vorticity in the water column [*Leth and Shaffer*, 2001], which added to the PCUC vorticity results in baroclinic instabilities that promote the formation of mesoscale eddies [*Colas et al*., 2012].

3.2. ITEs and Low-Frequency Internal Waves Off Central Chile

[12] Vertical sections of temperature, salinity, and dissolved oxygen in alongshore sections over the continental shelf margin (31–41°S), obtained during the cruises in the austral winter of 1997 and 2007, show a water tongue with high salinity (>34.5) and low dissolved oxygen (<1 mL L^{-1}), characteristics associated with the ESSW (shadowed areas in Figures 4b, 4d, 4f, and 4h). The region north of 36°S is dominated by the presence of the ESSW in the layer between 100 and 400 m depth, the layer of the PCUC. Southward of 36°S, the ESSW becomes progressively thinner towards the south, exhibiting a tongue centered at ∼200 m. Alongshore sections of salinity and dissolved oxygen are similar in both cruises (1997 and 2007); however, the sections of temperature and density show significant differences. Colder, denser, and less stratified waters were observed during the 2007 cruise. Temperature and density

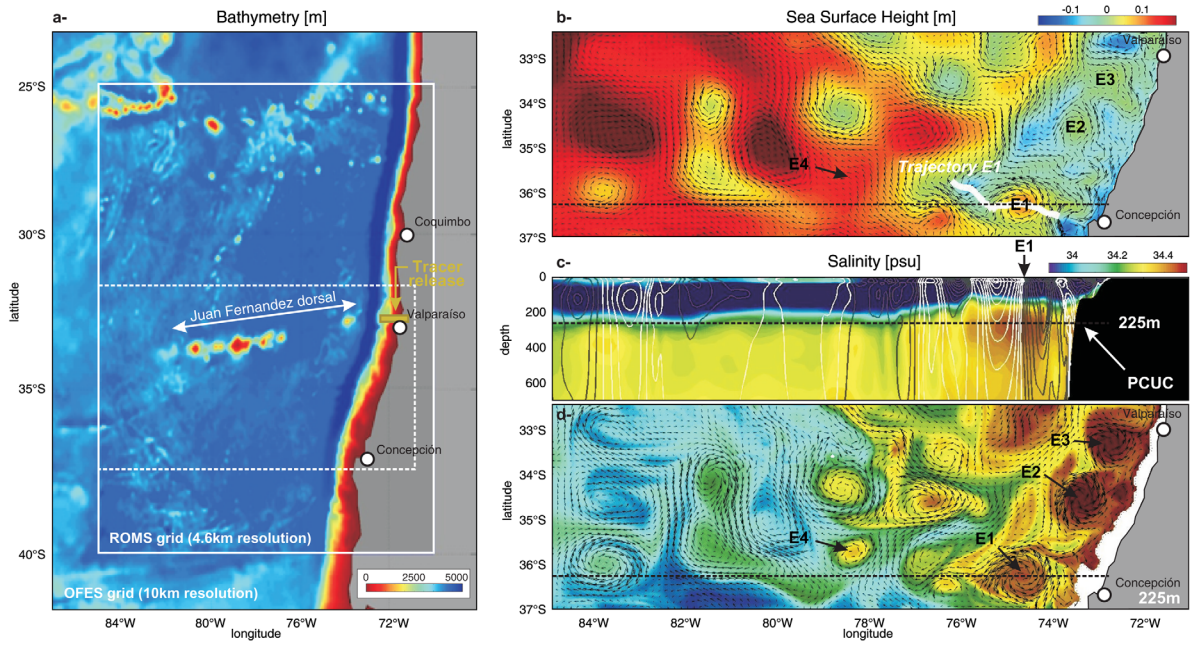

Figure 5. ROMS model—a snapshot of results for February 2007: (a) horizontal domain of the ROMS (~4.6 km resolution) and OFES (1/10° resolution) models, including the bathymetry (m) and the area where the passive tracer was released (between 150 and 400 m depth near Valparaiso, represented by a green box in Figure 5a). The results include (b) sea surface height (colour) and surface currents (arrows) in the area demarked by a white broken line in Figure 5a); (c) the vertical distribution of salinity (colour) and negative (white contour) and positive (black contour) meridional currents (0.03 m s^{-1} intervals) across Eddy 1 (E1; dashed line in Figure 5b)), located off Concepcion; (d) Horizontal distribution of salinity (color) and currents (arrows) at 225 m depth.

differences could be linked to interannual variability associated with ENSO. The 1997 cruise was carried out during one of strongest El Niño events [*McPhaden*, 1999], whereas the 2007 cruise took place during the initial phase of La Niña event [*Correa-Ramirez et al*., 2012]. During El Niño (La Niña), ITEs have a stronger (weaker) signal in the temperature and density fields, associated to warmer (colder) and saltier waters (Figure 4). During La Niña, the changes in the relative contribution of temperature and salinity to the density field results in a weaker density signal in ITEs. The ITEs that have a tendency to density compensation (variations in temperature and salinity without changes in density) could persist much longer, as observed for structures in scales smaller than the mesoscale [*Ferrari and Boccaletti*, 2004].

[13] The alongshore distribution of water properties revealed several areas where the ESSW was stretched (wider) and squeezed (narrower) in the vertical plane, represented by a shallowing (deepening) of the upper isolines and a deepening (shallowing) of the lower isolines (Figure 4). The vertical fluctuations of isolines in the water column along the continental shelf/slope areas (Figure 4) could correspond to low-frequency internal waves. In waters along the coast off Chile, the fluctuations in the vertical distribution of temperature below the base of the seasonal thermocline are relatively well represented by a single isotherm and these oscillations appear to be in phase with low-frequency internal waves [*Morales et al*., 1999;

Table 1. Mean Characteristics of Two Eddies Identified During the Austral Spring (1997) and Summer (2009) in the CTZ Off Central Chile

Eddy Characteristics	1997	2009
Area (diameter) during the cruise (km^2)	3839.6 (69.9)	5490.9 (83.6)
Area[a] [mean (std)] (km^2)	4616.7 (1419.3)	8369.7 (3748.7)
Shallower boundary[b] (m)	114.0	88.0
Deeper boundary[b] (m)	470.0	418.0
Thickness[c] (m)	356.0	330.0
Vorticity[d] [mean(std)] [1×10^{-6} s^{-1}]	5.70 (0.98)	6.81 (2.13)
Mean velocity (km d^{-1})	1.72	1.98
Azimut (°)	270	284
Total transport[e] (Sv)	0.76	1.19
ESSW transport[f] (Sv)	0.54	0.78
Life time (days)	49	322

[a]Mean and standard deviation of the surface area of eddies, from their coastal origin until their oceanic end. Areas were calculate from the enclosed polygons of the 1×10^{-12} threshold contour in the Okuvo Weiss field.
[b]Upper and bottom boundaries of the subsurface lenses delimited by the 34.5 psu salinity contour.
[c]Thickness of the subsurface lenses (upper minus bottom boundaries).
[d]Mean and standard deviation of the vorticity in the eddy's center through the life of the structures.
[e]Total transport obtained assuming a conservative total depth of 500 m. 1 Sv = 1×10^6 m^3 s^{-1}.
[f]Transport obtained using the lends thickness.

Blanco et al., 2002; *Montecinos and Pizarro*, 2005]. Also, it has been observed that the fluctuations in the vertical distribution of low oxygen waters, characteristic of the ESSW and which are well represented by the 1 mL L^{-1} isoline, are in phase with those of the isotherms and in opposite phase with sea level [*Morales et al*., 1999]. Accordingly, if the vertical fluctuation of isolines in the water column was due to low-frequency waves, the oscillation of the isolines of temperature, salinity, and oxygen located below the base of the thermocline should be in phase. In the present study, however, there was an opposite phase in the vertical fluctuation of the 11°C isotherm (representative of waters below the base of seasonal, upper thermocline) and that of salinity (34.5 isohaline) and dissolved oxygen (1 mL L^{-1} isooxycline), indicating that this pattern does not correspond to low-frequency waves.

[14] The areas where the ESSW was stretched (wider), forming a subsurface lens having an horizontal scale of ~100 km (bigger than the Rossby radius for the region, ~30 km), represent ITEs generated along the continental shelf/slope area. The distribution of water column properties in Figure 4 indicates that five to seven ITEs are simultaneously present in the CTZ between 31° and 38°S, area where Eddy Kinetic Energy (EKE) values have been previously found to be highest compared to the adjacent ones [*Hormazabal et al*., 2004]. The travel of ITEs through the CTZ in the region off central Chile could represent a mechanism by which low-oxygen waters in the ESSW are extended offshore. Although we cannot ascertain from these data that the five or seven ITEs observed were generated at the same time, a simultaneous formation of several ITEs as a response to baroclinic instabilities set up by shifts in wind direction has been previously reported for the Norwegian Sea [*Hansen et al*., 2010].

3.3. Model Results

[15] A numerical experiment for a passive tracer coupled to a ROMS model was performed in order to identify the origin of ITEs in the region off central Chile. The experiment consisted in the continuous release of a passive tracer in the PCUC (150–400 m depth) in the coastal area off Valparaiso (33°S) and in the analysis of the tracer distribution through time (Figure 5a). The results obtained from the model are exemplified for the austral summer in February 2007. Sea surface height (color) and surface geostrophic current field (arrows) during this period represented the features that are characteristic in the CTZ off central Chile, including a complex pattern of circulation with strong mesoscale eddy activity, meandering currents, and a coastal jet (Figure 5b). Among these structures, three anticyclonic eddies were distinguished in the area between Valparaiso and Concepcion (labeled as E1, E2, and E3 in Figure 5b). These structures were well represented by the tracer distribution in the horizontal plane at 225 m depth (Figure 6c). Also in the horizontal plane at 225 m depth, the areas containing maximum salinity cores and stronger currents in vortices confirmed the presence of the above eddies (Figure 5d). In addition, the model-derived eddy E1 was located in the same area of the trajectory of an ITE (white line in Figure 5b), which was detected during a summer cruise off Concepcion (Figure 3a).

[16] In the vertical plane (0–600 m depth), the distribution of the tracer concentration in a section from the coast to offshore at 36°20′S (dotted black line in Figures 5b and 5d) represented quite well the location of the PCUC and the presence of a subsurface mesoscale eddy (E1) with characteristics similar to an ITE (Figure 6c). The model-derived distributions of salinity and meridional currents (Figure 5c) also provided a realistic representation of the PCUC in this region (southward flow over the continental shelf/slope areas, containing a maximum in subsurface salinity, and with a core at ~225 m depth). Adjacent to the PCUC, a northward and a southward flow associated with the inshore and offshore boundaries of eddy E1, respectively, was also represented; water composition in this eddy was similar to that in the PCUC and very different from adjacent waters in the CTZ (Figure 5c). A closer view of the vertical distribution of water density in the area of eddy E1 (Figure 6a) showed that this structure had a vertical extension of ~500 m and a shape typical of an ITE: a dome in the upper part (100–160 m depth) and a bowl in the lower part (160–650

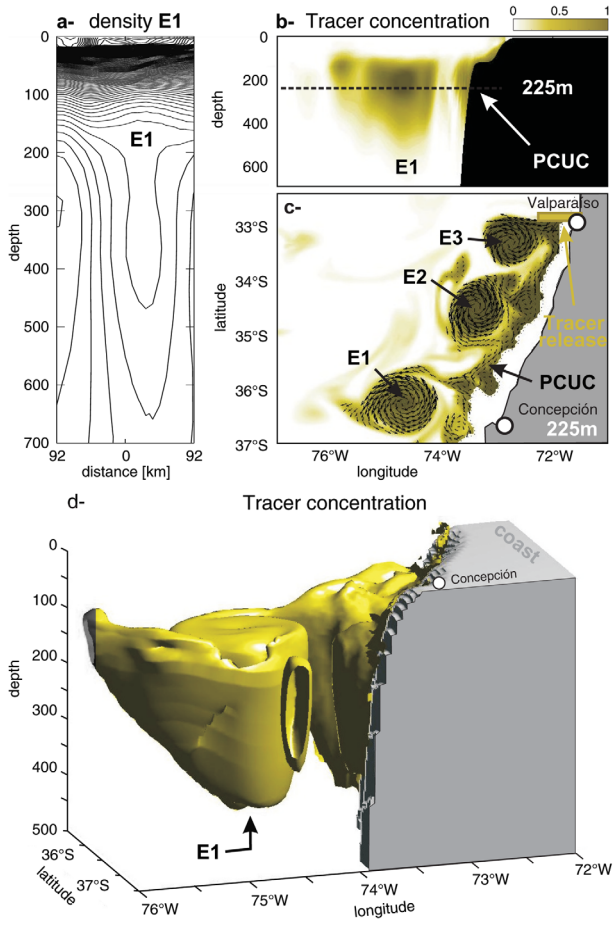

Figure 6. ROMS model—a snapshot of passive tracer results for February 2007. The passive tracer was released between 150 and 400 m depth, near Valparaiso (green box in Figure 6c). The results include (a) density anomaly profile across E1 (see also Figure 5c); (b) tracer concentration across E1; (c) horizontal distribution of tracer concentration (color) and currents (arrows) at 225 m depth (only currents associated to tracer were used); and (d) a 3D representation of the tracer off Concepcion (0.2 isocontour), denoting the detachment of E1 from the PCUC.

m). Other eddies generated with the model (E2 and E3 in Figures 5d and 6c) presented water column characteristics very similar to those of E1 (not shown), which suggested that they also corresponded to ITEs.

[17] A 3D representation of the tracer distribution in the area off Concepcion suggests that eddy E1 can be the result of a detachment from subsurface waters associated to the PCUC (Figure 6d). Thus, previous suggestions that ITEs in the region off central Chile are originated from the coastal poleward PCUC [*Johnson and McTaggart*, 2010; *Colas et al*., 2012] are supported by our model results. Wind forcing of coastal upwelling incorporates vorticity into the water column which, in addition to the vorticity of the PCUC, generates baroclinic instabilities that allow the formation of mesoscale eddies [*Leth and Shaffer*, 2001; *Colas et al*., 2012]. Some of these eddies correspond to ITEs, in which the geostrophic velocities are dominated by depression of the main pycnocline, and therefore, their rotation is anticyclonic, whereas the upward displacement of the seasonal pycnocline generates a cyclonic rotation in the surface layer [*McGillicuddy et al*., 2007]. The cyclonic ITEs will not survive for a long time because they will collapse under a destabilizing action of the horizontal surplus pressure gradient and the centrifugal and Coriolis forces [*Filyushkin and Sokolovskiy*, 2011].

[18] Based on the hydrographic and modeling results presented here, we propose that ITEs are regularly detached from the coastal region of central Chile, move mostly westward and slightly northward at speeds of $\sim$2 km d^{-1}, and have a volume transport on the order of $\sim$1 Sv (Table 1). This transport estimate is similar to that described for the PCUC off central Chile [*Shaffer et al*., 1999] and the mode value estimated from Argo float profiles for ITEs in this region [*Johnson and McTaggart*, 2010]. ITEs in this region have been described as being relatively infrequent away from the coastal area where they are generated [*Johnson and McTaggart*, 2010] and, therefore, it is quite a challenge to sample them at sea. No doubt that a modeling approach which includes the spatial and temporal variability in the generation of ITEs in this region will the next step to improve their characterization.

3.4. Impact of ITEs on the Pelagic System in the Region Off Central Chile

[19] Mesoscale eddies have been shown to influence, at least in part, the distribution or biomass of phytoplankton and zooplankton communities in the CTZ off central Chile. In particular, eddies have been shown to be sites of enhanced chlorophyll-a concentration in the CTZ but the mechanisms by which this is attained have remained unclear [*Correa-Ramirez et al*., 2007; *Morales et al*., 2007, 2010]. The offshore propagation of eddies in this region may contribute to extend toward the CTZ the area of high primary productivity found in the coastal upwelling band through the advection of phytoplankton biomass and nutrient-enriched waters. Additionally, some type of eddies can result in the upwelling of nutrients to the illuminated layers (through eddy pumping or other mechanisms) and, with it, can promote increases in phytoplankton biomass and phytoplankton production in the CTZ [*Correa-Ramirez et al*., 2007]. Recently, *Morales et al*. [2012] have shown that an ITE was a site of vertical injection of high nutrient concentrations from the ESSW into the upper layer in the CTZ and, probably, there was also ESSW nutrient advection involved.

[20] The effect of mesoscale eddies on the productivity in the CTZ of other eastern boundary current systems has been usually reported in positive terms, like the enhancement of chlorophyll-a within eddies compared with the surrounding waters [e.g., *Moore et al*., 2007; *Brzezinski and Washburn*, 2011; *Peterson et al*., 2011]. This positive effect in the CTZ, however, could be at the expense of diminishing the potential of fertilization of high nutrient waters during coastal upwelling. The modeling results of *Gruber et al*. [2011] suggest that eastern boundary current systems with higher eddy activity are associated with low level of biological production; their simulations show that eddies suppress production and also the downward export of organic matter is reduced through an eddy-induced transport of nutrients from the upwelling zone to the CTZ. *Morales et al*. [2012] have provided in situ evidence that this might be the case for ITEs.

[21] The impact of ITEs (because of their larger vertical dimension), as well as of other mesoscale eddies, in reducing the nutrient inventory in the coastal zone off central Chile remains to be assessed, and, for this to be achieved, a detailed characterization of the frequency of ITEs formation and of the dynamics during their early life history need to be available. On the other hand, the effects of ITEs in the enhancement of primary production in the CTZ could explain the distribution of some socioeconomically important natural resources. For example, a significant increase in the acoustic biomass of the highly migratory pelagic fish, jack-mackarel (*Trachurus symmetricus murphyi*), has been found in the area of the ITE identified during the fall of 1997 (Figure 2d). In addition, the larval stages of jack-mackarel have been found to be distributed mainly off central Chile [*Núñez et al*., 2004], where they likely find the most suitable food resources in association with the fertilizing effect of some eddy types. The distribution of demersal resources, which live in the oxygen minimum zone over the shelf and slope areas off central Chile, such as the Chilean hake (*Merluccius gayi*) [*San Martín et al*., 2011], could probably extend their distribution to the CTZ through ITEs. Moreover, ITEs probably reach the area of the subtropical gyre in the South Pacific [*Johnson and McTaggart*, 2010] and could act as a nutrient source for planktonic communities in this oligotrophic environment.

4. Concluding Remarks

[22] Hydrographic observations, satellite altimetry, and a ROMS model with a passive tracer coupled to this model were combined in order to study the origin and presence of mesoscale eddies of the ITE type. Results have shown that ITEs are recurrent features in the CTZ off central Chile (31–38°S), with five to seven simultaneously present along the CTZ adjacent to the coastal zone. These ITEs become detach from the PCUC, move mostly westward at average speeds of $\sim$2 km d^{-1} and produce a volume transport of $\sim$1 Sv. The main impact of ITEs is that, on one hand, they can act as main agents in the export offshore of coastally derived ESSW waters rich in nutrients and poor in oxygen, and, on the other hand, they can contribute to the expansion

toward the CTZ of the area of upwelling of ESSW waters and, with it, enhance the productivity of the system in the open ocean.

[23] **Acknowledgments.** Funds for this study were derived from CONICYT projects: FONDECYT 1070504 (CEM and SH) and FONDECYT 3110173 (MCR); part of the sampling and data were also supported by the following FIP projects: 96-13, 97-12, 2007-16, and 2008-20. S.H. was partially supported by the "Conservation, Research and Education Opportunities ("CREO") Program. The final stages of the writing of this manuscript were prepared under the support of the FONDECYT 1120504 project. The comments by two anonymous reviewers greatly improved the first version.

References

Ballegooyen, R. C., M. L. van Gründlingh, and J. R. E. Lutjeharms (1994), Eddy fluxes of heat and salt from the southwest Indian Ocean into the southeast Atlantic Ocean: A case study, *J. Geophys. Res*., *99*, 14,053–14,070, doi:10.1029/94JC00383.

Blanco, J. L., M.-E. Carr, A. C. Thomas, and P. T. Strub (2002), Hydrographic conditions off northern Chile during the 1996–1998 La Niño and El Niño events, *J. Geophys. Res., 107, C3*, doi:10.1029/2001JC001002.

Brzezinski, M. A., and L. Washburn (2011), Phytoplankton primary productivity in the Santa Barbara Channel: Effects of wind-driven upwelling and mesoscale eddies, *J. Geophys. Res.*, *116*, C12013, doi:10.1029/2011JC007397.

Cáceres, M. (1992), Vórtices y filamentos observados en imágenes satelitales frente al área de surgencia de Talcahuano, *Chile central, Invest. Pesq*., *37*, 55–66.

Capet, X., F. Colas, P. Penven, P. Marchesiello, and J. C. McWilliams (2008), *Eddies in Eastern-Boundary Subtropical Upwelling Systems, Geophys. Monogr. Ser., vol. 177, Eddy-Resolving Ocean Modeling*, 350 pp., AGU, Washington, D.C.

Chaigneau, A., G. Eldin, and B. Dewitte (2009), Eddy activity in the four major upwelling systems from satellite altimetry (1992–2007), *Prog. Oceanogr.*, *83*(1–4), 117–123, doi:10.1016/j.pocean.2009.07.012.

Chaigneau, A., M. Le Texier, G. Eldin, C. Grados, and O. Pizarro (2011), Vertical structure of mesoscale eddies in the eastern South Pacific Ocean: A composite analysis from altimetry and Argo profiling floats, *J. Geophys. Res.*, *116*, C11025, doi:10.1029/2011JC007134.

Colas, F., J. McWilliams, X. Capet, and J. Kurian (2012), Heat balance and eddies in the Peru-Chile current system, *Clim. Dyn.*, *39*(1), 509–529, doi:10.1007/s00382-011-1170-6.

Combes, V., E. Di Lorenzo, and E. Curchitser (2009), Interannual and decadal variations in cross-shelf transport in the Gulf of Alaska, *J. Phys. Oceanogr.*, *39*(4), 1050–1059, doi:10.1175/2008JPO4014.1.

Correa-Ramirez, M. A., S. Hormazabal, and G. Yuras (2007), Mesoscale eddies and high chlorophyll concentrations off central Chile (29°-39°S), *Geophys. Res. Lett.*, *34*, L12604, doi:10.1029/2007GL029541.

Correa-Ramirez, M. A., S. Hormazabal, and C. E. Morales (2012), Spatial patterns of annual and interannual surface chlorophyll-a variability in the Peru-Chile Current System, *Prog. Oceanogr.*, *92-95*, 8–17, doi:10.1016/j.pocean.2011.07.008.

da Silva, A. M., C. C. Young, and S. Levitus (Eds.) (1994), Atlas of Surface Marine Data 1994, vol. 1, Algorithms and Procedures, NOAA Atlas NESDIS, vol. 6, 83 pp., NOAA, Silver Spring, Md., *NOAA Atlas Nesdis*, *6*(83), 20910–3282.

Dugan, J. P., R. P. Mied, P. C. Mignerey, and A. F. Schuetz (1982), Compact, intrathermocline eddies in the Sargasso Sea, *J. Geophys. Res.*, *87*, 385–393, doi:10.1029/JC087iC01p00385.

Ferrari, R., and G. Boccaletti (2004), Eddy-mixed layer interactions in the ocean, *Oceanography*, *17*(3), 12–21, doi: 10.5670/oceanog.2004.26.

Filyushkin, B. N., and M. A. Sokolovskiy (2011), Modeling the evolution of intrathermocline lenses in the Atlantic Ocean, *J. Mar. Res.*, *69*(2-3), 191–220, doi:10.1357/002224011798765231.

Garfield, N., C. A. Collins, R. G. Paquette, and E. Carter (1999), Lagrangian exploration of the California undercurrent, 1992–95, *J. Phys. Oceanogr.*, *29*(4), 560–583, doi:10.1175/1520-0485(1999)029<0560:LEOTCU>2.0.CO;2.

Gordon, A. L., C. F. Giulivi, C. M. Lee, H. H. Furey, A. Bower, and L. Talley (2002), Japan/East Sea intrathermocline eddies, *J. Phys. Oceanogr.*, *32*(6), 1960–1974, doi:10.1175/1520-0485(2002)032<1960:JESIE>2.0.CO;2.

Gruber, N., Z. Lachkar, H. Frenzel, P. Marchesiello, M. Münnich, J. C. McWilliams, T. Nagai, and G.-K. Plattner (2011), Eddy-induced reduction of biological production in eastern boundary upwelling systems, *Nat. Geosci.*, *4*(11), 787–792, doi:10.1038/ngeo1273.

Haidvogel, D. B., H. G. Arango, K. Hedstrom, A. Beckmann, P. Malanotte-Rizzoli, and A. F. Shchepetkin (2000), Model evaluation experiments in the North Atlantic Basin: Simulations in nonlinear terrain-following coordinates, *Dyn. Atmos. Oceans*, *32*(3–4), 239–281, doi:10.1016/S0377-0265(00)00049-X.

Hansen, C., E. Kvaleberg, and A. Samuelsen (2010), Anticyclonic eddies in the Norwegian Sea: Their generation, evolution and impact on primary production, *Deep Sea Res. Part I*, *57*(9), 1079–1091, doi:10.1016/j.dsr.2010.05.013.

Hormazabal, S., G. Shaffer, and O. Leth (2004), Coastal transition zone off Chile, *J. Geophys. Res.*, *109*, C01021, doi:10.1029/2003JC001956.

Isern-Fontanet, J., J. Font, E. Garcia-Ladona, M. Emelianov, C. Millot, and I. Taupier-Letage (2004), Spatial structure of anticyclonic eddies in the Algerian basin (Mediterranean Sea) analyzed using the Okubo-Weiss parameter, *Deep Sea Res. Part II*, *51*(25-26), 3009–3028.

Jerónimo, G., and J. Gómez-Valdés (2007), A subsurface warm-eddy off northern Baja California in July 2004, *Geophys. Res. Lett.*, *34*, L06610, doi:10.1029/2006GL028851.

Johnson, G. C., and K. E. McTaggart (2010), Equatorial Pacific 13°C water eddies in the Eastern Subtropical South Pacific Ocean, *J. Phys. Oceanogr.*, *40*(1), 226–236, doi:10.1175/2009JPO4287.1.

Kostianoy, A. G., and I. M. Belkin (1989), A survey of observations on intrathermocline eddies in the world ocean, in *Mesoscale/Synoptic Coherent Structures in Geophysical Turbulence, Elsevier Oceanogr. Ser*., vol. *50*, edited by J. C. J. Nihoul and B. M. Jamart, pp. 821–841, Elsevier, Amsterdam.

Letelier, J., O. Pizarro, and S. Nuñez (2009), Seasonal variability of coastal upwelling and the upwelling front off central Chile, *J. Geophys. Res.*, *114*, C12009, doi:10.1029/2008JC005171.

Leth, O., and G. Shaffer (2001), A numerical study of seasonal variability in the circulation of central Chile, *J. Geophys. Res.*, *106*, 22,229–22,248.

Leth, O., and J. F. Middleton (2004), A mechanism for enhanced upwelling off central Chile: Eddy advection, *J. Geophys. Res.*, *109*, C12020, doi:10.1029/2003JC002129.

Marchesiello, P., J. C. McWilliams, and A. Shchepetkin (2001), Open boundary conditions for long-term integration of regional oceanic models, *Ocean Modell.*, *3*(1–2), 1–20, doi:10.1016/S1463–5003(00)00013-5.

Martin, A. P., and K. J. Richards (2001), Mechanisms for vertical nutrient transport within North Atlantic mesoscale eddy, *Deep Sea Res., Part II*, *48*, 757–773.

Masumoto, Y., et al. (2004), A fifty-year eddy-resolving simulation of the World Ocean—Preliminary outcomes of OFES (OGCM for the Earth simulator), *J. Earth Simul.*, *1*, 31–52.

McDowell, S. E., and H. T. Rossby (1978), Mediterranean water: An intense mesoscale eddy off the Bahamas, *Science*, *202*(4372), 1085–1087, doi:10.1126/science.202.4372.1085.

McPhaden, M. J. (1999), Genesis and evolution of the 1997-98 El Niño, *Science*, *283*, 950–954, doi:10.1126/science.283.5404.950.

McGillicuddy, D. J., et al. (2007), Eddy/wind interactions stimulate extraordinary mid-ocean plankton bloom, *Science*, *316*(5827), 1021–1026.

Mellor, G. L., T. Ezer, and L.-Y. Oey (1994), The pressure gradient conundrum of sigma coordinate ocean models, *J. Atmos. Oceanic Technol.*, *11*(4), 1126–1134, doi:10.1175/1520-0426(1994)011<1126:TPGCOS>2.0.CO;2.

Montecinos, A., and O. Pizarro (2005), Interdecadal sea surface temperature–sea level pressure coupled variability in the South Pacific Ocean, *J. Geophys. Res.*, *110*, C08005, doi:10.1029/2004JC002743.

Moore, T. S., II, R. J. Matear, J. Marra, and L. Clementson (2007), Phytoplankton variability off the Western Australian Coast: Mesoscale eddies and their role in cross-shelf exchange, *Deep Sea Res., Part II*, *54*(8–10), 943–960, doi:10.1016/j.dsr2.2007.02.006.

Morales, C. E., S. Hormazabal, and J. L. Blanco (1999), Interannual variability in the mesoscale distribution of the depth of the upper boundary of the oxygen minimum layer off northern Chile (18–24°S): Implications for the pelagic system and biogeochemical cycling, *J. Mar. Res.*, *57*, 909–932.

Morales, C. E., H. Gonzalez, S. Hormazabal, G. Yuras, J. Letelier, and L. Castro (2007), The distribution of chlorophyll-a and dominant planktonic components in the coastal transition zone off concepcion, central

Chile, during different oceanographic conditions, *Prog. Oceanogr.*, *75*(3), 452–469, doi:10.1016/j.pocean.2007.08.026.

Morales, C. E., M. Loreto Torreblanca, S. Hormazabal, M. Correa-Ramírez, S. Nuñez, and P. Hidalgo (2010), Mesoscale structure of copepod assemblages in the coastal transition zone and oceanic waters off central-southern Chile, *Prog. Oceanogr.*, *84*(3-4), 158–173, doi:10.1016/j.pocean.2009.12.001.

Morales, C. E., S. Hormazabal, M. Correa-Ramirez, O. Pizarro, N. Silva, C. Fernandez, V. Anabalón, and M. L. Torreblanca (2012), Mesoscale variability and nutrient–phytoplankton distributions off central-southern Chile during the upwelling season: The influence of mesoscale eddies, *Prog. Oceanogr.*, *104*, 17–29, doi:10.1016/j.pocean.2012.04.015.

Nauw, J. J., H. M. van Aken, J. R. E. Lutjeharms, and W. P. M. de Ruijter (2006), Intrathermocline eddies in the Southern Indian Ocean, *J. Geophys. Res.*, *111*, C03006, doi:10.1029/2005JC002917.

Núñez, S., J. Letelier, D. Donoso, A. Sepúlveda, and D. Arcos (2004), Relating spatial distribution of Chilean jack mackerel and environmental factors in the oceanic waters off Chile, *Gayana*, *68*(2), 444–449, doi:10.4067/S0717-65382004000300023.

Peterson, T. D., D. W. Crawford, and P. J. Harrison (2011), Evolution of the phytoplankton assemblage in a long-lived mesoscale eddy in the eastern Gulf of Alaska, *Mar. Ecol. Prog. Ser.*, *424*, 53–73, doi:10.3354/meps08943.

Pizarro, O., and A. Montecinos (2004), Interdecadal variability of the thermocline along the west coast of South America, *Geophys. Res. Lett.*, *31*, L20307, doi:10.1029/2004GL020998.

Richardson, P. L., A. S. Bower, and W. Zenk (2000), A census of Meddies tracked by floats, *Prog. Oceanogr.*, *45*, 209–250.

San Martín, M. A., L. A. Cubillos, and J. C. Saavedra (2011), The spatio-temporal distribution of juvenile hake (Merluccius gayi gayi) off central southern Chile (1997–2006), *Aquat. Living Resour.*, *24*, 161–168, doi:10.1051/alr/2011120.

Sasaki, H., Y. Sasai, S. Kawahara, M. Furuichi, F. Araki, A. Ishida, Y. Yamanaka, Y. Masumoto, and H. Sakuma (2004), A series of eddy-resolving ocean simulations in the world ocean: OFES (OGCM for the Earth Simulator) project, *OCEAN'04*, *3*, 1535–1541.

Sasaki, H., M. Nonaka, Y. Masumoto, Y. Sasai, H. Uehara, and H. Sakuma (2006), An eddy-resolving hindcast simulation of the quasi-global ocean from 1950 to 2003 on the Earth Simulator, in *High Resolution Numerical Modelling of the Atmosphere and Ocean*, edited by W. Ohfuchi and K. Hamilton, pp. 157–185, Springer, New York.

Shaffer, G., S. Hormazabal, O. Pizarro, and S. Salinas (1999), Seasonal and interannual variability of currents and temperature off central Chile, *J. Geophys. Res.*, *104*, 29,951–29,961.

Shapiro, G. I., and S. L. Meschanov (1991), Distribution and spreading of Red Sea Water and salt lens formation in the northwest Indian Ocean, *Deep Sea Res. A*, *38*(1), 21–34, doi:10.1016/0198-0149(91)90052-H.

Shchepetkin, A. F., and J. C. McWilliams (2005), The regional oceanic modeling system (ROMS): A split-explicit, free-surface, topography-following-coordinate oceanic model, *Ocean Modell.*, *9*(4), 347–404, doi:10.1016/j.ocemod.2004.08.002.

Silva, N., and S. Neshyba (1979), On the southernmost extension of the Peru-Chile undercurrent, *Deep Sea Res. Part A*, *26*(12), 1387–1393, doi:10.1016/0198-0149(79)90006-2.

Silva, N., N. Rojas, and A. Fedele (2009), Water masses in the Humboldt current system: Properties, distribution, and the nitrate deficit as a chemical water mass tracer for Equatorial subsurface water off Chile, *Deep Sea Res. II*, *56*(16), 1004–1020, doi:10.1016/j.dsr2.2008.12.013.

Simpson, J. J., and R. J. Lynn (1990), A mesoscale eddy dipole in the offshore California Current, *J. Geophys. Res.*, *95*, 13,009–13,022, doi:10.1029/JC095iC08p13009.

Treguier, A. M., J. Deshayes, C. Lique, R. Dussin, and J. M. Molines (2012), Eddy contributions to the meridional transport of salt in the North Atlantic, *J. Geophys. Res.*, *117*, C05010, doi:10.1029/2012JC007927.